

Transient Electromagnetic Behavior of Multiply Contacted Interconnects

Peter Böhm, Gerhard Wachutka

Institute for Physics of Electrotechnology, Munich University of Technology
Arcisstr. 21, D-80290 Munich, Germany, boehm@tep.ei.tum.de

ABSTRACT

This paper presents a methodology for the analysis of the transient electromagnetic behavior of multiply contacted interconnects.

It is shown that for applications with high switching frequencies and high pulse repetition rates with subsequent steep current ramps, the usual characterization of interconnects by extracting an inductance matrix based on a static current distribution is not sufficient and has to be extended or even replaced by the determination of distributed transient fields and the specification of time-dependent characteristic quantities.

It is demonstrated that only a full three-dimensional transient analysis under realistic switching conditions can give the necessary insight in the time-dependent behavior of the electric and magnetic fields in- and outside the interconnects.

The method is illustrated by an example encountered in an industrial high power application.

Keywords: Distributed Parasitic Effects, Interconnects, Finite Element Method, Transient Analysis.

INTRODUCTION

The electromagnetic behavior of interconnects is usually described by an inductance matrix consisting of the self and mutual inductance coefficients. This is done on the basis of the magnetostatic approximation, assuming a quasi-stationary current distribution, which can be easily determined for even complex geometries using the Poisson equation, or in the time-harmonic domain where the skin effect is included. For these cases, a well-established method exists, namely the Partial-Element-Equivalent-Circuit method [1], which is based on determining partial inductances by evaluating Neumann's formula.

However, there are applications where the transient character of the electromagnetic dynamical behavior cannot be neglected, such as for high switching frequencies and high pulse repetition rates with subsequent steep current ramps. These applications can be found in various fields and gain more and more importance.

As there is also a pronounced trend to shortening switching times, we have developed a methodology for

the analysis of the full time-dependent electromagnetic behavior of interconnects. It includes the treatment of distributed parasitic effects, in particular time-dependent inductive effects, eddy currents and current crowding phenomena. Primarily developed for high power applications where switching times of some 100 ns or even shorter, and switched currents in the range of one kilo-ampere have become feasible, this analysis method can also be applied to the field of microdevices with much shorter switching times and less high current values but comparable pulse slopes.

Moreover, it has been demonstrated that only a full three-dimensional transient simulation under realistic switching conditions can reproduce the real world behavior. The knowledge of the time-dependent electromagnetic fields inside and outside the interconnects and of derived quantities, e. g. the resulting current distribution, allows the minimization of distributed parasitics and therefore the improvement of the interconnects by shape optimization.

THEORY

We start with the time-dependent Maxwell equations using a scalar potential φ which represents the quasi-static contribution to the electric field in the conducting region(s), and a vector potential \vec{A} for the magnetic field in- and outside the conducting region(s). The governing equation in quasi-stationary approximation, which excludes the formation of electromagnetic waves, becomes

$$\operatorname{rot} \frac{1}{\mu} \operatorname{rot} \vec{A} + \sigma \dot{\vec{A}} = -\sigma \operatorname{grad} \varphi, \quad (1)$$

subjected to Coulomb's gauge $\operatorname{div} \vec{A} = 0$ as constraint. Normally used to ensure the uniqueness of the magnetic vector potential \vec{A} and for numerical stability, it is additionally used here to decouple the potentials φ and \vec{A} . We can therefore separate the governing equation into a Laplace equation

$$\operatorname{div} (\sigma \operatorname{grad} \varphi) = 0 \quad (2)$$

to calculate the quasi-stationary potential-driven current contribution $\vec{j}_{qs} = -\sigma \operatorname{grad} \varphi$ and a kind of diffusion equation

$$\frac{\partial \vec{A}}{\partial t} - \frac{1}{\mu \sigma} \Delta \vec{A} = -\nabla \varphi \quad (3)$$

to determine the vector potential \vec{A} . Having calculated the potentials φ and \vec{A} , the total current density is obtained by

$$\vec{j} = \vec{j}_{qs} + \vec{j}_{ind} = -\sigma \text{grad}\varphi - \sigma \dot{\vec{A}} \quad (4)$$

To deal with problems of multiply contacted interconnects, we build up the quasi-stationary current flow from basis functions, using a separation of space and time variables

$$\vec{j}_{qs}(\vec{r}, t) = \sum_{k, \alpha} \vec{j}_{k\alpha}(\vec{r}) I_{k\alpha}(t), \quad (5)$$

where α denotes a single part of an interconnect structure and k a single contact on the interconnect part α (Fig. 1).

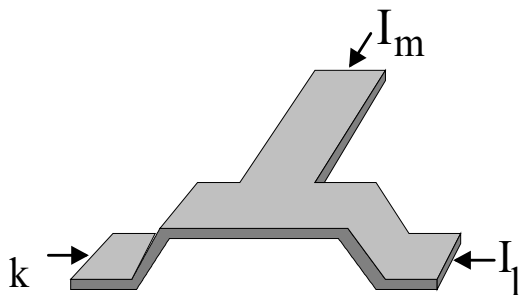


Figure 1: Multiply contacted interconnect

Using the analogue decomposition of the magnetic vector potential,

$$\vec{A}(\vec{r}, t) = \sum_{k, \alpha} \int \vec{A}_{k\alpha}(\vec{r}, t - \tau) I_{k\alpha}(\tau) d\tau \quad (6)$$

the resulting current distribution can be expressed as the sum of a source current density \vec{j}_{qs} and an induced current density \vec{j}_{ind} , related to each contact electrode $C_{k\alpha}$.

$$\begin{aligned} \vec{j}(\vec{r}, t) &= \sum_{k, \alpha} \vec{j}_{k\alpha}(\vec{r}) I_{k\alpha}(t) \\ &\quad - \sigma_{\alpha} \int \vec{A}_{k\alpha}(\vec{r}, t - \tau) \dot{I}_{k\alpha}(\tau) d\tau \end{aligned} \quad (7)$$

Evaluating the magnetic field energy in terms of the terminal currents $I_{k\alpha}(t)$, we find that a time-dependent inductance matrix can be extracted:

$$\begin{aligned} L_{k\alpha, l\beta}(\tau) &= \int_{\Omega_{\alpha}} \vec{j}_{k\alpha}(\vec{r}) \vec{A}_{l\beta}(\vec{r}, \tau) d^3r \\ &= \frac{1}{\sigma_{\alpha}} \langle \vec{j}_{k\alpha} | e^{-\mathcal{D}\tau} \vec{j}_{l\beta} \rangle \end{aligned} \quad (8)$$

where $\mathcal{D} = \frac{1}{\mu\sigma} \Delta$.

Based on these quantities and with a view to shape optimization, we are able to define target functionals to assess the quality of a given interconnect set-up with respect to the uniformity of current flow, switching time delay, overvoltage and overheating limitations and related quantities of interest.

EXAMPLE

As an illustrative example, we discuss fast transient effects in a double-plate structure encountered in an industrial application. The simulation is based on the $\vec{A}, V\text{-}\vec{A}$ formalism [2]. $\vec{A}, V\text{-}\vec{A}$ stands for solving the vector and scalar potentials (\vec{A}, φ) inside the conducting region(s) and \vec{A} in the nonconducting region(s). The finite element simulation is based on classical node-elements, where the uniqueness of the potentials (\vec{A}, φ) is ensured by a penalty term $-\nabla \cdot \frac{1}{\mu} \nabla \cdot \vec{A}$ at the left-hand side of (1) and by choosing a special setup of interface conditions along the boundaries of the conducting parts of the simulation domain. This allows a differentiation between the potential driven quasi-stationary current flow and the induced eddy currents mentioned in equation (4) and (7).

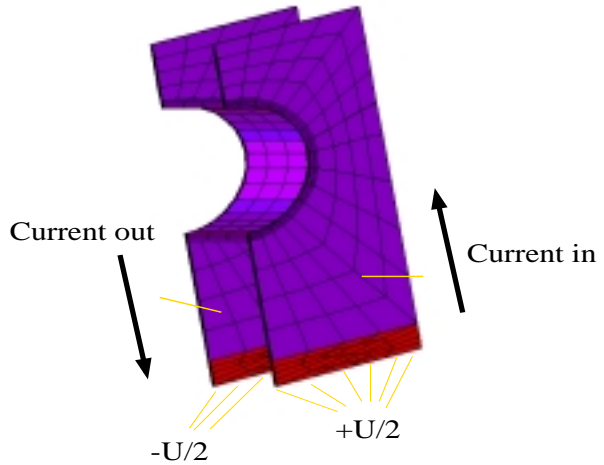


Figure 2: Double-plate structure, consisting of two parallel plates connected by a perpendicular sheet-metal. The densely meshed, red colored regions at the open end of the plates represent areas with increased resistivity. The vertical dimensions of the double-plate structure are stretched by a factor of 25.

The double-plate structure consists of two parallel copper plates with a circular cut, having a length and

width in the range of centimeters and being separated by a dielectric layer of two millimeters. They are connected by a perpendicularly attached curved sheet-metal. The two layers themselves have a thickness of $100\mu\text{m}$ (Fig. 2).

Additional high resistive layers at the open ends of the plates are used to reconcile the entire current flow with the absolute value of the applied voltage. The open ends of the structure are connected to a virtual voltage source by using Dirichlet boundary-conditions. The voltage was ramped up at the contact electrodes with a pulse rise-time of 100ns and maintaining the maximum value afterwards (Fig. 3).

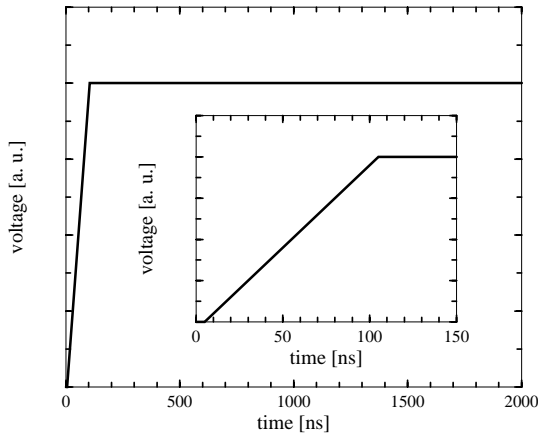


Figure 3: Voltage ramp used as bias condition for the transient simulation of current turn-on

Because of the steep voltage ramp, all quantities characterizing the interconnects are affected by the electromagnetic dynamical behavior of the interconnect.

As expected, induced eddy currents lead to a dramatic redistribution of the current densities in the interconnect. Because of the antiparallel current flow through the plates, the current density is enlarged along the inner side of the sandwich, whereas it is reduced along the outer side. Furthermore, we find pronounced current crowding at the source bound side of the curved perpendicular plate, leading to an additional inhomogeneity of the current density and a significantly higher heating rate (Fig. 4).

Considering the quasi-stationary current flow $\vec{j} = -\sigma\nabla\varphi$ through the contact electrodes, which is driven by the voltage drop across the interconnects, allows us to analyse the turn-on transients of the terminal currents passing the contact electrodes. Because their behavior is mainly determined by the inductances of the interconnects, we would expect a behavior similar to that of a simple RL-network. This idea is clearly confirmed by figure 5. The square-dotted line represents the ideal

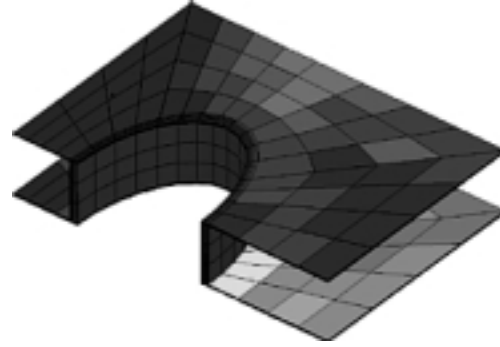


Figure 4: Current distribution inside the interconnect at a time step half way during turn-on (light grey: high, dark grey: low current density).

case, where all inductances are assumed to be zero and the terminal current can be expressed by $I = U/R_{static}$. Therefore, the current follows the voltage ramp and reaches its maximum value at the end of the ramp.

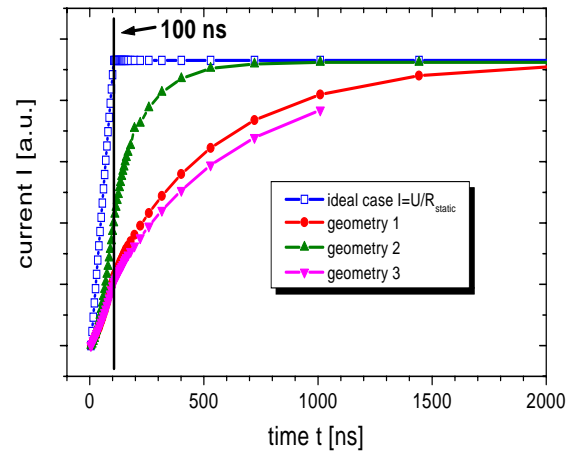


Figure 5: Current flow through the contact electrodes driven by the voltage drop across the interconnect for different geometries.

The three other lines show that a variation of the geometrical shape of the interconnects leads to different inductances and, thereby, influences the turn-on time of the module. It can be seen that for geometry one and three it takes about two microseconds (or twentieth the ramp-time) to reach a quasi-stationary state.

It also turned out that even minor changes of the geometry could strongly influence the inductivity. This is therefore the dominant factor which limits the switching frequency and determines switching losses.

Like other quantities, the inductance becomes a function of time. By decomposing the voltage drop into an ohmic and an inductive contribution, it is possible to extract time-dependent inductance values for each step of the simulation (Fig. 6). Again, the inductivity is strongly depending on the geometry of the interconnect.

All results are corroborated by experimental data and give us valuable insight with a view to an optimized design.

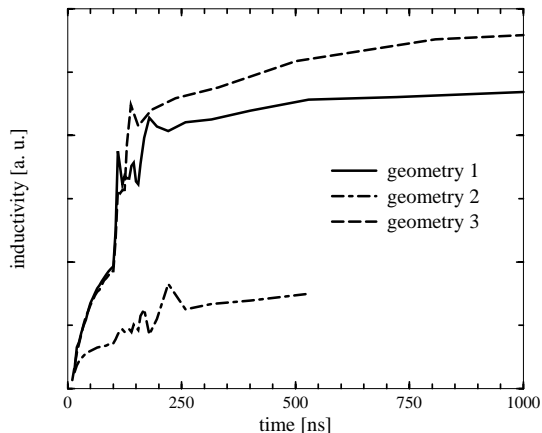


Figure 6: Simulated time-dependent inductance of the interconnect for different geometries

FUTURE PERSPECTIVES

Equipped with the evaluation and visualization of the electromagnetic fields inside and outside the interconnects, we are able to optimize interconnects under transient switching conditions by parameter studies. For the given target functional L_{tot} , we can formulate an optimization problem

$$L_{tot}(\tau_{opt}) = \inf_{\tau \in U_{ad}} L_{tot}(\tau), \quad (9)$$

where U_{ad} denotes the design parameter space.

For example, if we want to minimize the global inductivity, we have to find

$$\inf_{\sigma, \mathcal{G}} L(\sigma, \mathcal{G}; \varphi(\sigma, \mathcal{G}), \vec{A}(\sigma, \mathcal{G})), \quad (10)$$

where \mathcal{G} stands for the geometry and σ for the conductivity of the interconnect. This equation has to be solved under certain constraints, e. g. that \vec{A} and φ solve the field equations. This requires fast and stable algorithms and solvers for the $\vec{A}, V\text{-}\vec{A}$ -field problem, which are at the moment not yet available but under development. As a final result we note that the time-dependent inductance matrix evaluated by (8) can be used as a transient input for a circuit simulation.

REFERENCES

- [1] Ruehli, A.E.: Inductance Calculation in a Complex Integrated Circuit Environment . IBM-Journal of Research and Development (1972) 470–481
- [2] Bíró, O., Preis, K.: On the Use of the Magnetic Vector Potential in the Finite Element Analysis of Three-Dimensional Eddy Currents. IEEE Trans. Mag. **25** (1989) 3145–3159